CrystEngComm

Accepted Manuscript

ROYAL SOCIETY OF CHEMISTRY

www.rsc.org/crystengcomm

Structural Diversity and Luminescent Properties of Coordination Polymers Based on Mixed Ligands, 2,5-Bis(Imidazol-1-yl)Thiophene ($Thim_2$) and Aromatic Multicarboxylates

Namita Singh and Ganapathi Anantharaman*

Department of Chemistry, Indian Institute of Technology (IIT), Kanpur – 208016, INDIA.

Email: garaman@iitk.ac.in.

Abstract

Seven new CPs $\{[Zn(thim_2)(o\text{-}BDC)]\cdot(H_2O)_2\}_n$ (**1**), $[Co(thim_2)(m\text{-}BDC)]_n$ (**2**), $\{[M(thim_2)(HBTC)]\cdot(H_2O)\}_n$ [M=Co(**3**) and Zn(**4**)], $\{[M(thim_2)(OBA)]\cdot(H_2O)_2\}_n$ [M= Co(**5**) and Zn(**6**)], $[Mn_2(thim_2)_2(m\text{-}BDC)_2(H_2O)]_n$ (**7**) [o-H_2BDC= phthalic acid, m-H_2BDC= isophthalic acid, H_3BTC= trimesic acid, H_2OBA= 4,4'oxybis(benzoic acid)] have been prepared by hydro/solvothermal reaction of different metal salts with 2,5-bis(imidazol-1-yl)thiophene ($thim_2$) in presence of various multicarboxylic acids. CP **1** exhibits a 2D herringbone pleated network structure. CP **2** reveals a 2D+2D= 3D polycatenated framework composed of 2D parallel pleated network. CPs **3** and **4** show isostructural 2D herringbone pleated network. CPs **5** and **6** are also isostructural and form 2D layer structure which are arranged in $\cdots ABAB \cdots$ pattern in crystal lattice. CP **7** forms a 3D framework consisting of 1D $[Mn_2(m\text{-}BDC)_2(H_2O)]_n$ chains which are linked by $thim_2$. The structures of all five type of CPs indicate that different multicarboxylate coligands play an important role in structural variation. Thermal stability of all the CPs (**1**-**7**) was monitored by TGA. Furthermore solid state photoluminescence was investigated for **1**, **4** and **6** at room temperature.

Introduction:

Coordination polymers (CPs) have seized the considerable attention because of their interesting architecture and topologies as well as their promising applications in the field of gas adsorption, heterogeneous catalysis, magnetism and photoluminescence.[1-5] The appropriate selection of the metal ion and organic ligand are the key factors which can effectively control the structural diversity in CPs. Also other experimental factors like solvent, anion, reaction temperature, reaction time, and pH have significant influence on the crystal structure besides the supramolecular interactions.[6] Furthermore, a new strategy has been introduced for tuning the structure of CPs using the mixed ligand systems, such as a combination of multicarboxylic acids as auxiliary units with N-donor ligands or vice versa.[7] Multitopic N-donor ligands, with linear, semi-rigid or flexible coordinating mode, have been marked as a good candidate for assembling CPs. As compared to the large pillaring effect of linear N-donor ligands in the structures of CPs, a wide range of complex structural assemblies of CPs, such as honeycombs, cages, and interpenetrated networks, have been reported with multitopic flexible ligands since they can adopt various conformations while coordinating to the metal ion.[8] In contrast semi-rigid ligands, in particular three five-membered rings, have not been well exploited. Also rigid and flexible multicarboxylic organic ligands can be used for the construction of novel structures because of their diverse coordination modes, after being completely or partially deprotonated, and different orientations of the carboxylate groups.[9] Moreover, number and position of the carboxylate group (positional isomers) in the moiety can influentially modulate the structure leading to the formation of varying and interesting networks.[10] In this context we have focused on the angular three five-membered heterocyclic rings 2,5-bis(imidazol-1-yl)thiophene ($thim_2$) which has the special characteristics of changing the conformation through C-N bond rotation between the

thiophene and terminal imidazolyl group when connected to the metal center. Thus it was predicted that combining this angular ligand with rigid or flexible aromatic coligands (Scheme 1) can lead to rational formation of interesting structural architectures and topologies.

In addition to the structural diversity, CPs based on transition metal ion or lanthanide ion and functional organic ligands provide a suitable platform for the synthesis of luminescence materials.[11] CPs as luminescent material have been vastly explored and have been found applicable in photo chemistry, electrochemical display, sensing and optical devices.[11a, 12] Various type of π conjugated organic moieties such as organothiophenes and phenyl ring based ligands are adequate to show luminescent properties.[13] Besides, d^{10} metal ion such as zinc and cadmium are prone to show luminescence enhancement and do not quench the luminescence like paramagnetic transition metal ions.

Initially, we have investigated the structural diversity of CPs synthesized using $thim_2$ with various metal sulphates.[14] In continuation, in this paper we have reported the seven new CPs $\{[Zn(thim_2)(o\text{-}BDC)]\cdot(H_2O)_2\}_n$ (**1**), $[Co(thim_2)(m\text{-}BDC)]_n$ (**2**), $\{[M(thim_2)(HBTC)]\cdot(H_2O)\}_n$ [M=Co(**3**) and Zn(**4**)], $\{[M(thim_2)(OBA)]\cdot(H_2O)_2\}_n$ [M= Co(**5**) and Zn(**6**)], $[Mn_2(thim_2)_2(m\text{-}BDC)_2(H_2O)]_n$ (**7**) synthesized using $thim_2$ and various co-ligands with different metal salts. Their structural properties have been discussed along with infrared spectra (IR), powder X-Ray diffraction (PXRD) and thermo gravimetric analysis (TGA). In addition the fluorescence properties of CPs **1**, **4** and **6** have been investigated in solid state.

Experimental Section

Materials and physical measurements.

2,5 dibromo thiophene, CuI, trimesic acid (H_3BTC) (Sigma Aldrich) and 4,4'oxybis(benzoic acid) (H_2OBA) (Alfa Aesar) as well as other chemicals such as anhyd. K_2CO_3, imidazole,

phthalic acid (o-H_2BDC), isophthalic acid (m- H_2BDC), and metal salts (sd fine-cHEM. Ltd.) were obtained and used as received. Solvents were received, from sd fine-cHEM. Ltd., and purified by standard procedures prior to use.[15] Thim$_2$ was prepared according to the reported literature procedure.[14] Infrared spectra (IR) were recorded using KBr pellet on Perkin–Elmer model 1320 spectrometer in the range of 4000-400 cm^{-1}. Thermogravimetric analysis (TGA) was performed under nitrogen atmosphere (heating rate of 5^{o}C/min) on Mettler Toledo star system. Microanalyses for all the compounds were collected using Perkin Elmer Series-II 2400 Elemental Analyzer. Solid state emission spectra were performed on Jobin Yvon Horiba Fluorolog-3 spectrofluorimeter at room temperature. Powder X-ray diffraction spectra (CuK_α radiation, scan rate 3^o/min, 293 K) were collected on a Bruker D8 advance series 2 Powder X-ray diffractometer.

Single-Crystal X-ray Studies.

Single crystal X-ray data were recorded at 100 K on a Bruker SMART APEX CCD diffractometer using graphite-monochromated MoK_α radiation (λ= 0.71073 Å). SAINT software was used for data integration and reduction.[16] Absorption correction was performed with SADABS. All the structures were solved by the direct method employing SHELXS-97 and SHELXL-97 was used to refine on F^2 with full-matrix least squares technique.[17] All hydrogen atoms were fixed in idealized position using a riding model. Non hydrogen atoms were refined anisotropically. The hydrogen atoms of water molecules were located from difference Fourier maps and the DFIX command was used to constrain the O-H bond distances (~0.90 Å). The disordered water molecules present in the channel of CPs **5** and **6**, were treated by squeeze refinement using PLATON.[18] All the squeezed water molecules have been included in the empirical formula as well as formula weight of the respective CP.

Synthesis of {[Zn(thim$_2$)(o-BDC)]·(H$_2$O)$_2$}$_n$ (1)

A mixture of Zn(OOCCH$_3$)$_2$·2H$_2$O (0.022 g, 0.1 mmol), thim$_2$ (0.021g, 0.1 mmol), and o-H$_2$BDC (0.016g, 0.1 mmol) in H$_2$O (7 mL) was sealed in Teflon lined autoclave and heated to 160 ^{o}C for 72 h and gradually cooled down to room temperature. The colorless crystals were obtained. Yield: 0.032 g (66.66%, based on Zn(OOCCH$_3$)$_2$·2H$_2$O Anal. Calcd for $C_{18}H_{16}N_4O_6SZn$: C, 44.87; H, 3.34; N, 11.62% Found: C, 45.50; H, 3.03; N, 11.37%. IR (KBr, cm^{-1}) 3512(m), 3390(m), 3146(w), 3085(m), 1607(vs), 1575(vs), 1541(m), 1526(m), 1498(s), 1443(w), 1374(vs), 1309(s), 1261(m), 1216(w), 1150(w), 1126(m), 1113(m), 1084(w), 1052(s), 947(s), 921(w), 848(m), 803(s), 759(s), 708(w), 650(s), 590(w), 534(w), 482(w), 421(w).

Synthesis of [Co(thim$_2$)(m-BDC)]$_n$ (2)

The same reaction procedure was used as for **1** except that Zn(OOCCH$_3$)$_2$·2H$_2$O and o-H$_2$BDC were replaced by Co(OOCCH$_3$)$_2$·4H$_2$O (0.025 g, 0.1 mmol) and m-H$_2$BDC (0.016g, 0.1 mmol). The dark purple color crystals were obtained. Yield: 0.025 g (56.81%, based on Co(OOCCH$_3$)$_2$·4H$_2$O) Anal. Calcd for $C_{18}H_{12}N_4O_4SCo$: C, 49.21; H, 2.75; N, 12.75% Found: C, 48.62; H, 2.58; N, 12.31%. IR (KBr, cm^{-1}) 3134(m), 3115(m), 3074(m), 1607(vs), 1580(s), 1558(vs), 1490(s), 1473(m), 1448(w), 1347(vs), 1318(vs), 1255(m), 1243(m), 1201(w), 1152(w), 1112(s), 1103(m), 1074(w), 1053(vs), 943(m), 921(w), 897(w), 858(w), 838(w), 828(m), 791(m), 763(m), 744(m), 733(vs), 722(vs), 673(w), 661(m), 648(s), 622(w), 570 (w), 558(m), 544(m).

Synthesis of {[Co(thim$_2$)(HBTC)]·(H$_2$O)}$_n$ (3)

The same reaction procedure was used as for **1** except that Zn(OOCCH$_3$)$_2$·2H$_2$O and o-H$_2$BDC were replaced by Co(OOCCH$_3$)$_2$·4H$_2$O (0.025 g, 0.1 mmol) and H$_3$BTC (0.021 g, 0.1 mmol). The dark purple color crystals were obtained. Yield: 0.021 g (42.00%, based on

$Co(OOCCH_3)_2 \cdot 4H_2O$ Anal. Calcd for $C_{19}H_{14}N_4O_7SCo$: C, 45.51; H, 2.81; N, 11.17% Found: C, 44.98; H, 2.76; N, 10.68%. IR (KBr, cm^{-1}) 3492(br), 3128(m), 2638(w), 2546(w), 1878(w), 1702(s), 1622(vs), 1575(s), 1534(m), 1495(m), 1435(s), 1382(w), 1341(vs), 1289(vs), 1210(m), 1110(s), 1099(m), 1069(w), 1050(s), 1034(m), 942(m), 923 (w), 905(w), 867(w), 814(m), 793(m), 751(s), 728(s), 701(s), 676 (w), 650(s), 620(w), 572(w), 555(m), 488(w), 468(w), 427(w).

Synthesis of $\{[Zn(thim_2)(HBTC)]\cdot(H_2O)\}_n$ (4)

A mixture of $Zn(NO_3)_2 \cdot 6H_2O$ (0.030 g, 0.1 mmol), $thim_2$ (0.021 g, 0.1 mmol) and H_3BTC (0.021 g, 0.1 mmol) in DMF/H_2O (2 mL/1 mL) was sealed in Teflon lined autoclave and heated to 90 ^oC for 72 h and gradually cooled down to room temperature. The colorless crystals were obtained. Yield: 0.027 g (52.94%, based on $Zn(NO_3)_2 \cdot 2H_2O$) Anal. Calcd for $C_{19}H_{14}N_4O_7SZn$: C, 44.94; H, 2.77; N, 11.03% Found: C, 44.79; H, 2.67; N, 10.76%. IR (KBr, cm^{-1}) 3491(br), 3130(m), 2873(w), 2546(w), 1702(s), 1626(vs), 1577(vs), 1536(m), 1497(m), 1433(m), 1340(vs), 1290(vs), 1243 (w), 1212(w), 1192(w), 1112(m), 1100(m), 1069(w), 1051(s), 1035(m), 944(m), 924(w), 906(w), 866(w), 813(w), 793(w), 752(s), 729(s), 701(s), 677(w), 650(s), 622(w), 571(w), 554(m), 487(w), 463(w).

Synthesis of $\{[Co(thim_2)(OBA)]\cdot(H_2O)_2\}_n$ (5)

The same reaction procedure was used as for **1** except that $Zn(OOCCH_3)_2 \cdot 2H_2O$ and o-H_2BDC were replaced by $Co(OOCCH_3)_2 \cdot 4H_2O$ (0.025 g, 0.1 mmol) and H_2OBA (0.026 g, 0.1 mmol). The dark purple color crystals were obtained. Yield: 0.021 g (37.5 %, based on $Co(OOCCH_3)_2 \cdot 4H_2O$ Anal. Calcd for $C_{24}H_{20}N_4O_7SCo$: C, 50.79; H, 3.55; N, 9.87% Found: C, 51.25; H, 3.14; N, 10.45%. IR (KBr, cm^{-1}) 3417(br), 3116(m), 2535(w), 1683(m), 1595(vs), 1578(s), 1495(s), 1418(s), 1402(s), 1369(s), 1306(s), 1250(s), 1230(vs), 1201(m), 1161(s),

1111(m), 1064(w), 1047(m), 1030(m), 1011(m), 947(m), 940(m), 923(w), 901(w), 881(m), 872(m), 856(m), 832(w), 813(w), 799(w), 778(m), 769(m), 730(m), 711 (w), 696(w), 663(m), 652(s), 620(w), 545(m), 523(w), 501(w), 488(w).

Synthesis of $\{[Zn(thim_2)(OBA)]\cdot(H_2O)_2\}_n$ (6)

The same reaction procedure was used as for **4** except that H_3BTC was replaced by H_2OBA (0.026 g, 0.1 mmol). The colorless block shaped crystals were obtained. Yield: 0.025 g (43.85%, based on $Zn(NO_3)_2\cdot 6H_2O$ Anal. Calcd for $C_{24}H_{18}N_4O_6SZn$ (**6**-H_2O): C, 52.46; H, 3.30; N, 10.19 % Found: C, 52.78; H, 3.14; N, 10.45%. IR (KBr, cm^{-1}) 3443(br), 3134(m), 1712(w), 1668(w), 1604(vs), 1574(s), 1537(m), 1495(s), 1414(m), 1370(vs), 1328(m), 1307(m), 1228(vs), 1204(m), 1161(m), 1093(m), 1065(w), 1049(m), 1031(m), 1010(w), 949(m), 942(m), 923(w), 902(w), 871(m), 854(m), 801(m), 780(m), 768 (w), 732(m), 711(w), 696(w), 672(w), 663(w), 652(m), 620(w), 544(w), 523(w), 485(w).

Synthesis of $[Mn_2(thim_2)_2(m\text{-}BDC)_2(H_2O)]_n$ (7)

The same reaction procedure was used as for **1** except that $Zn(OOCCH_3)_2\cdot 2H_2O$ and o-H_2BDC were replaced by $Mn(OOCCH_3)_2\cdot 4H_2O$ (0.024 g, 0.1 mmol) and m-H_2BDC (0.016g, 0.1 mmol). The pale yellow color crystals were obtained. Yield: 0.023 g (53.48 %, based on $Mn(OOCCH_3)_2\cdot 4H_2O$ Anal. Calcd for $C_{36}H_{26}N_8O_9S_2Mn_2$: C, 48.65; H, 2.94; N, 12.60% Found: C, 48.67; H, 2.76; N, 12.33%. IR (KBr, cm^{-1}) 3411(br), 3111(m), 3088(m), 1610(s), 1573(s), 1543(s), 1489 (m), 1428(m),1380(vs), 1306(m), 1262(w), 1235(w), 1209(w), 1154(w), 1101(m), 1073(w), 1048(s), 928(m), 899(w), 852(m), 827(m), 809(m), 780 (w), 739(s), 722(s), 700 (m), 673(w), 655(m), 617(w), 549(w), 414(w).

RESULT AND DISCUSSION

All the CPs were synthesized under hydrothermal (**1**-**3**, **5** and **7**)/solvothermal (**4** and **6**) conditions and found stable in air, insoluble in water and common organic solvents. All the CPs (**1**-**7**) were analyzed using IR, elemental analysis and single crystal X-ray diffraction methods. A broad peak between 3400-3500 cm^{-1} was observed for CPs (**1** and **3**-**7**) corresponding to the coordinated or uncoordinated water molecules. IR spectra of (**1**-**6**) shows the ($\nu_{as(OCO)}$ and $\nu_{s(OCO)}$) characteristics absorption peaks at 1607(vs) cm^{-1} and 1374(vs) cm^{-1} for **1**, 1607(vs) cm^{-1} and 1347(vs) cm^{-1} for **2**, 1622(vs) cm^{-1} and 1341(vs) cm^{-1} for **3**, 1626(vs) cm^{-1} and 1340(vs) cm^{-1} for **4**, 1595(vs) cm^{-1} and 1369(vs) cm^{-1} for **5**, 1604(vs) cm^{-1} and 1370(vs) cm^{-1} for **6**. The observed $\Delta\nu$ suggests monodentate coordination mode of carboxylate groups to the metal ions. In addition there is a strong peak observed at 1702 cm^{-1} that corresponds to the C=O of the carboxylic group indicating the presence of protonated carboxylic acid moiety. Also CP **7** display multiple carboxylate stretching frequencies, $\nu_{as(OCO)}$ and $\nu_{s(OCO)}$ for carboxylate groups at 1610(vs) cm^{-1}, 1543(vs) cm^{-1} and 1428(s) cm^{-1}, 1380(vs) cm^{-1} respectively which suggest more than one type of coordination modes to the manganese ion.[19] Elemental analysis of CPs (**1**-**7**) shows 1:1 composition of $thim_2$ and aromatic carboxylates in the final structures.

Single-crystal X-ray structure of CPs 1-7

Structure analysis of $\{[Zn(thim_2)(o\text{-}BDC)]\cdot(H_2O)_2\}_n$ (1)

The single crystal x-ray analysis reveals that **1** crystallizes in monoclinic $P2_1/n$ space group (Table 1) and asymmetric unit consists of one Zn(II) ion, one $thim_2$, one o-BDC anion and one water molecule in the lattice. Zinc ion is tetra-coordinated with N_2O_2 donor set and adopts distorted tetrahedral geometry. The two nitrogen atoms are provided by the two imidazoles of two different $thim_2$ ligands and the remaining two oxygen atoms are provided by two different o-

BDC anions (Figure 1a). $Thim_2$ ligand connects the two metal centers through imidazolyl nitrogen atoms along b direction to generate the 1D-helical chain. Within each $thim_2$ ligand, the imidazole rings are twisted and the dihedral angle between two imidazolyl rings is 48.48(9)º. The zinc ions in these chains are linked by different carboxylate groups of o-BDC in monodentate connecting mode, resulting a 2D network (Figure 1b). The two carboxylate groups in o-BDC attain different orientation with 58.72 (1)º dihedral angle. Within the 2D network all the metal atoms are not coplanar, half of the metal atoms fall in one plane and other half in another parallel plane. Considering the connectivity between each Zn ion to $thim_2$ and o-BDC units, the structure **1** belongs to a 2D herringbone pleated (first order) network as shown in Figure 1c. The dimension of $[Zn_4(thim_2)_2(o\text{-}BDC)_2]$ rhombic grid within the 2D network is 7.28 Å × 12.55 Å (Figure 1c). These 2D networks are well separated and are linked through C–H···O interactions along *c* direction in ··*AA*·· fashion to form a 3D supramolecular network [Table S2 and Figure 1d].

The Zn–N [2.014(4) Å and 2.018(5) Å] and Zn–O [1.949(4) Å and 1.971(4) Å] bond distances in **1** are found comparable with the reported Zn–N [2.000(2) Å and 2.014(2) Å] and Zn–O [1.959(3) Å and 1.981(3) Å] bond distances in similar imidazole and o-BDC bound CPs.[20]

Structure analysis of $[Co(thim_2)(m\text{-}BDC)]_n$ (2)

Single crystal x-ray study shows that CP **2** crystallizes in chiral orthorhombic space group $P2_12_12_1$ (Table 1). The asymmetric unit contains one cobalt ion, one $thim_2$ and one m-BDC ligand. Like **1**, the cobalt ion adopts a distorted tetrahedral geometry surrounded by two monodentate carboxylate belonging to two m-BDC ligands and two imidazole nitrogen atoms from two different $thim_2$ ligands (figure 2a). The cobalt ions are connected through imidazole nitrogen atoms of $thim_2$ to form a 1D helical chain. Further, each cobalt ion in the chains are

linked by carboxylates of m-BDC in mono-dentate coordination mode resulting in the formation of a 2D parallel pleated like network (Figure 2b and 2c). Unlike **1**, the dihedral angle between two imidazolyl rings within each $thim_2$ is 87.01(9)º whereas, the dihedral angle between two coordinated carboxylate to cobalt ion is 12.77 (1)º. The 2D network is composed of $[M_4(thim_2)_2(m\text{-}BDC)_2]$ grids with the dimension of 10.14 × 12.19 Å (Figure 2c). In 2D network metal carboxylate chains are not coplanar, adjacent chains lie in the different parallel plane while alternate one fall in same plane which are connected by $thim_2$ ligands and impart the parallel pleated like pattern to whole 2D network. These 2D layers are entangled by two parallel adjacent 2D layers (one upper and one lower) where $thim_2$ ligands of one layer pass through the two adjacent layers and leads the formation of 2D + 2D = 3D polycatenated framework (Figure 2d).

The Co–N/O bond distances are Co(1)–N(1) = 2.040(3) Å, Co(1)–N(4)= 2.046(3) Å, Co(1)–O(2)= 1.966(2) Å, Co(1)–O(3) = 2.015(3)Å. The bond distances are found comparable with Co–N av. [2.027(1) Å] and Co–O [1.973(6) Å, 2.016(2) Å] in similar type coordinated metal imidazole and BDC anion.[21]

Structure analysis of $\{[M(thim_2)(HBTC)]\cdot(H_2O)\}_n$ [M= Co (3) and Zn (4)]

The X-ray structural determination reveals that **3** and **4** crystallize in monoclinic crystal lattice with $P2_1/n$ space group and they are isostructural (Table 1). Hence, the structure of **3** alone is discussed here. The asymmetric unit is composed of one cobalt ion, one $thim_2$ ligand, one HBTC anion and one water molecule in the lattice. As in **2**, the cobalt ion exhibits distorted tetrahedral geometry involving N_2O_2 donor set. The metal ion is ligated with two imidazole nitrogen atoms from two different $thim_2$ units and two oxygen atoms from two carboxylate groups of two different HBTC (Figure 3a). Each $thim_2$ binds the metal ion through imidazole nitrogen atoms [Co(**3**), Zn(**4**)] to form a 1D helical chains. The metal ions in the 1D chains are further

connected by the carboxylate groups in monodentate connecting mode to form a 2D herringbone pleated (first order) network as shown in (Figure 3b, 3c). Within each $thim_2$ ligand dihedral angle between two imidazolyl rings is 66.31(8)º (**3**) and 60.32(2)º (**4**). The dihedral angle between two coordinated carboxylate is 20.76 (2)º (**3**) and 17.31(6)º(**4**). Among the three carboxylic acid groups in H_3BTC ligand only two of them are deprotonated in reaction medium, and coordinated to the metal centers while the another one remains as such. The 2D layer is composed of $[M_4(Hbtc)_2(thim_2)_2]$ [M= Co(**3**), Zn(**4**)] rhombic grids with dimension of 9.07 × 12.40 Å (**3**) and 9.18 ×12.40 Å (**4**) (Figure 3c). Similar to **1**, the metal atoms in the 2D network are not coplanar, half metal atoms fall in the one plane and other half in another parallel plane. The 2D layers are arranged one over another in ··*AA*·· manner through hydrogen bonding and supramolecular interactions to form 3D network along *a* direction (Figure 3d). The free carboxylic acid of trimesic acid in a layer is having a hydrogen bonding interaction with the free carboxylic acid group present in the fourth layer and form a well known hydrogen bonded carboxylic acid dimer (Figure S1, Table S3).

The bond distances M–N [Co, 2.017(5) Å, 2.044(5) Å and Zn, 1.986(5) Å, 2.017(6)Å] and M–O [Co, 1.967(5) Å, 1.995(4)Å] are observed similar to the reported M–N [Co, av. 2.016(3) Å and Zn, av. 2.009(5)Å] and M–O [Co, av. 2.009(2) Å and Zn, av. 1.989(5)Å] bond distances in imidazole and BTC binded CPs.[22]

Structure analysis of $\{[M(thim_2)(OBA)]\cdot(H_2O)_2\}_n$ [M= Co (5) and Zn (6)]

The X-ray structural analysis reveals that CPs **5** and **6** possess isostructural framework, therefore only the structure of **5** is discussed here. CP **5** crystallizes in monoclinic *C*2/*c* space group (Table 1). The asymmetric unit consists of one Co(II) ion, one $thim_2$, one OBA ligand and two water molecules in the lattice. The Co(II) ion is tetra-coordinated with two imidazole N atoms from

two different $thim_2$ ligand and two oxygen atoms from two monodentate carboxylate groups of two different OBA ligand. The coordination geometry surrounding cobalt ion can be described as distorted tetrahedral. (figure 4a). Like previously, the $thim_2$ and OBA connect the metal centers through nitrogen atoms of two imidazoles and oxygen atoms of two carboxylate moieties in mono-dentate coordination mode respectively to form a 2D network (Figure 4b). Within each $thim_2$ ligand dihedral angle between two imidazolyl rings is 72.25(3)º (**5**) and 74.29(4)º (**6**). Also unlike **2** and **3**, all cobalt ions are present in one plane. The dimensions of the $[M_4(thim_2)_2(OBA)_2]$ [M= Co(**5**), Zn(**6**)] rhombic grid in the 2D network is 12.18 × 13.81 Å (**5**) and 12.09 × 13.90 Å (**6**) (Figure 4c). These 2D networks are linked through C–H···O supramolecular interactions in ····*ABAB*···· fashion (Figure 4c) and generates a packed 3D supramolecular architecture [(Table S2) (Figure 4d, 4e)].

The M–N [Co, 2.033(4) Å, 2.051(4)Å and Zn, 2.010(3) Å, 2.041(3)Å] and M–O bond distances [Co, 1.978(4) Å, 1.998(4)Å and Zn, 1.963(3) Å, 1.963(2) Å] are found consistent with M–N [Co av.2.027(1) Å and Zn av. 2.033(5)] and M–O [Co av. 1.994(5) Å and Zn av. 1.984(4) Å]bond distances in metal imidazole and carboxyate bonded CPs.[21, 23]

Structure analysis of $[Mn_2(thim_2)_2(m\text{-}BDC)_2(H_2O)]_n$ (7)

The single crystal x-ray analysis reveals that **7** crystallizes in triclinic space group *P*-1 (Table 1) and asymmetric unit consists of crystallographically independent two manganese ions (Mn1 and Mn2), two $thim_2$ ligands, two m-BDC anions and one coordinated water molecule. Mn1 shows distorted octahedral geometry coordinated by four oxygen atoms from three m-BDC ligands in the plane and two nitrogen atoms from two different $thim_2$ axially. Whereas, Mn2 is coordinated by four equatorial oxygen atoms belonging from one water molecule (O9W) and three m-BDC units while axial sites of Mn2 are coordinated by two nitrogen atoms from imidazole of two

$thim_2$ ligands (Figure 5a). Interestingly, there are three different kinds of carboxylate binding modes of m-BDC to the manganese ions, which are responsible for its observed multiple IR stretching frequencies. The carboxylates of one of the m-BDC unit involved in chelating (Mn1) and bridging bidentate (Mn1 and Mn2) coordination modes to two different manganese ions which is getting extended to form a 1D chain. Such two 1D chains run anti-parallel to each other along *b* direction. Whereas, the carboxylate groups of another m-BDC adopt mono-dentate (Mn2) and bridging bidentate coordination mode and connects the two chains, running anti-parallel, to form a 1D double chain like structure (Figure 5b and 5c). Further each manganese ion of this 1D double chain is linked by the imidazole nitrogen atoms of $thim_2$ axially which connect each chain to four neighboring chains to form a 3D network (Figure S2, 5d).

Interestingly, the multiple coordination modes of carboxylate groups to the manganese ion within 1D network generated three different dimeric units of variable ring size with the composition of $[Mn_2C_2O_4]$, $[Mn_2C_{10}O_4]$ and $[Mn_2C_{12}O_4]_2$. The Mn-O bonding distances are found in the range of 2.125(3) -2.350(3) Å. The Mn-N bond distances also fall in ranges of 2.238(3)-2.273(3) Å). All the Mn–N/O bond distances are found consistent with other similar CPs.[24]

Influence of $thim_2$ ligand and Coligands in Structural Diversity of CPs (1-6)

The different structures of CPs (**1-7**) illustrate the influence of metal ion geometry and different multicarboxylate co-ligands in presence of common $thim_2$ ligand. Among the multicarboxylic acids used in the current work, three differed by the position and number of carboxylic acid groups (o-BDC, m-BDC and H_3BTC), whereas the rest one, H_2OBA, is a dicarboxylic acid containing flexible skeleton. The distance between the two metal centres linked by the $thim_2$ is influenced by the dihedral angle between the imidazole rings. While the distance between

carboxylate groups linked metal ions is affected by the position of carboxylate groups as well as dihedral angle between coordinated carboxylates. In CPs **1**-**6** the metal ion adopts tetrahedral geometry with N_2O_2 donor set coordinated by carboxylate and $thim_2$ linker. As shown in the Table 2, barring the difference between the metal ions in CP **1** and **2**, the distance between the metal center increases from 7.28 Å (**1**) to 10.14 Å (**2**). Also, the dihedral angle between mono-dentate carboxylate group bound to the metal ion decreases as the distance between metal centre increases. However, these effects were less significant in the case of isostructural CPs **3** and **4**. If one compares the CPs **1**-**4**, one can see that increasing in the dihedral angle of bound carboxylate moiety decreases the distance between the metal ions. Moreover the metal carboxylate chains are also changing from non-linear (**1**-**4**) to the linear like chain. (**3**). Similarly, as the dihedral angle between the imidazoles of $thim_2$ increases the distance between the metal ions decreases (**1**-**4**), but this effect is opposite to that of carboxylate dihedral angle. Thus, the observed structures in CPs (**1**-**4**) can be correlated with the combined effect of dihedral angles of ligand and coligands as well as distances between the metal ion. For instance, the polycatanation in **2** is favored because of smaller dihedral angle between carboxylates (and more in case of $thim_2$) and increased distance between the metal ion. Whereas, in the remaining three CPs (**1**, **3** and **4**) the larger carboxylate dihedral angle (less in case of $thim_2$) and decreased distanced between metal ions resulted in herringbone pleated 2D network. As noticed above, in CPs **1**-**4** metal-metal distance reduces as the dihedral angle between imidazole groups increases but in **5** and **6** decreasing of the dihedral angle of $thim_2$ increases the metal-metal distance. This change could be occured due to the flexibility of the dicarboxylate moiety and leads to the formation of 2D layer.

TGA and PXRD analysis.

The thermal stability of all the CPs (**1-7)** was examined using TGA under nitrogen atmosphere. TGA plot of **1** display the weight loss (calculated 7.4 % ; observed 7.6 %) for two lattice water molecules between 35-165 ^{o}C and dehydrated compound shows stability upto 290 ^{o}C (Figure S3). CP **2** exhibits the stability upto 380 ^{o}C and above this CP begins to decompose (Figure S4). CP **3** show a weight loss (calculated 3.6 %; observed 3.8 %) between the 35 to120 ^{o}C corresponding to the removal of lattice water molecule. The dehydrated framework show stability upto 360 ^{o}C (Figure S5). The TGA curve of **4** shows loss of lattice water molecule (calculated 3.5%; observed 3.3%) between 35 to 120 ^{o}C and framework was stable upto 320 ^{o}C (Figure S6). CP **5** show a weight loss (calculated 6.3 %; observed 6.5 %) between the 30 to 140 ^{o}C corresponding to the removal of lattice water molecule and framework show stability upto 390 ^{o}C (Figure S7). For **6** weight loss (calculated 6.2%, observed 6.1%) of two lattice water molecules occurs between 30-160 ^{o}C and complex show stability upto 340 ^{o}C (Figure S8). For **7**, a weight loss (calculated 2.0 %; observed 1.7 %) corresponding to the removal of coordinated water molecule was observed between 180-250 ^{o}C and resultant structure was found stable upto 325 ^{o}C (Figure S9). The experimental spectra of PXRD match with the corresponding simulated spectra for all **1-7** CPs which assure the bulk sample purity (Figure S10-S16).

Luminescent properties:

The CPs based on d^{10} transition metal ion and functional organic ligand have been reported as promising luminescent materials since both the moieties (metal ion and ligand) can play important role in generating luminescence.[25] Luminescence properties such as emission wave length of ligand obtain different after coordination to the metal ion due to the higher stability of ligand in CP.[26] Emission properties of CPs (**1, 4** and **6**) were investigated in the solid

state at room temperature. The luminescent emission spectra of $thim_2$ and CPs (**1, 4** and **6**) are depicted collectively in Figure 6. For $thim_2$ an emission band obtained at 400 nm (λ_{ex} = 260 nm).[14] In addition H_2-oBDC, H_3BTC and H_2OBA display emission peaks at 353 nm (λ_{ex} = 281 nm), 363 nm (λ_{ex} = 300 nm) and 317 nm (λ_{ex} = 276 nm) respectively These emission can be assigned due to the π*- π and π*-n transitions.[7a, 27] CPs (**1, 4** and **6**), exhibit an enhanced strong emission band at 370 nm (λ_{ex} = 260 nm) (**1**), 391 nm (λ_{ex} = 268 nm) (**4**) and 395 nm (λ_{ex} = 250nm) (**6**) respectively. These emission spectra show the resemblance with free ligand spectra however small blue shift was observed in wavelength maxima of all CPs. Such difference in emission behavior might be originated due to difference in coligand, crystal packing and coordination angle of the ligand in each coordination polymer. Therefore the ligand resembles luminescence profile with small blue shift could be attributed to the intra-ligand charge transfer transitions. As depicted in the figure 6 that CPs show enhancement in the luminescence intensity compared to the ligand. Among them **1** show highest intensity followed by **4** and the least enhancement is observed for **6**. This intensity enhancement may be caused by the ligand coordination to metal center which increase the rigidity of the ligand within CP which reduces the loss of energy by radiation less decay.[28]

Conclusion:

In conclusion we have synthesized and structurally characterized seven new Mn(II)/Co(II)/Zn(II) ion containing CPs fabricated by $thim_2$ and rigid/flexible benzene multicarboxylate under hydro/solvothermal conditions. 2D and 3D networks of CPs show interesting structural features such as herringbone pleated (first order) network of **1**and **3**-**4,** 3D poly-catanated network of **2** composed of 2D parallel pleated network, 2D rhombic grid network of **5**-**6** and 3D network of **7**. The structural variation in all the CPs demonstrates the significant role of the multicarboxylate

coligands and metal ion geometry along with ligand $thim_2$. Moreover position and orientation of the coordinated carboxylate groups as well as flexibility of the ligand are important factors to tune the structure of CPs. Thermal stability of all CPs (**1**-**7**) in which **5** shows highest stability and a strong luminescence enhancement was observed for **1** and **3**. Further influence of more conjugated multicarboxylate systems with different metal ions in the presence of $thim_2$ are under progress.

ASSOCIATED CONTENT

SUPPORTING INFORMATION

Additional figures, TGA, Powder X-ray diffraction patterns. X-ray crystallographic data in CIF format have been deposited with the Cambridge Structural Database (CCDC 941030, 925604, 995790, 912259, 941031, 995791, 945449).

AUTHOR INFORMATION

Corresponding author

*E-mail: garaman@iitk.ac.in

ACKNOWLEDGMENTS

The authors thank the Council of Scientific and Industrial Research (CSIR), and Department of Science and technology (DST), Government of India for their financial support and the Indian Institute of Technology (IIT), Kanpur for infrastructural facilities. NS thank University Grant Commission (UGC) for providing fellowship to do doctoral study.

References

1. (a) N. Stock and S. Biswas, *Chem. Rev.*, 2012, **112**, 933; (b) M. O'Keeffe and O. M. Yaghi, *Chem. Rev.* , 2012, **112**, 675; (c) S. R. Batten, S. M. Neville and D. R. Turner, *Coordination Polymers Design, Analysis and Application*, *RSC*, 2009. (d) C. Janiak, *Dalton Trans.*, 2003, 2781.

2. (a) F O. K. Farha, A. O. Yazaydin, I. Eryazici, C. D. Malliakas, B. G. Hauser, M. G. Kanatzidis, S. T. Nguyen, R. Q. Snurr and J. T. Hupp, *Nat. Chem.*, 2010, **2**, 944; (b) J. R. Li, R. J. Kuppler and H. Zhou, *Chem. Soc. Rev.*, 2009, **38**, 1477.

3. (a) M. Yoon, R. Srirambalaji and K. Kim, *Chem. Rev.*, 2012, **112**, 1196; (b) L. Ma, J. M. Falkowski, C. Abney and W. Lin, *Nat. Chem.*, 2010, **2**, 838; (c) A. Corma, H. García and F. X. Llabrés i Xamena, *Chem. Rev.*, 2010, **110**, 4606; (d) D. Farrusseng, S. Aguado and C. Pinel, *Angew. Chem. Int. Ed.*, 2009, **45**, 7502.

4. (a) M. Kurmoo, *Chem. Soc. Rev.*, 2009, **38**, 1353; (b) D. Maspoch, D. Ruiz-Molina and J. Veciana, *J. Mater. Chem.*, 2004, **14**, 2713.

5. Y. Cui, Y. Yue, G. Qian and B. Chen, *Chem. Rev.*, 2012, **112**, 1126.

6. (a) K. P. Rao, M. Higuchi, J. Duan and S. Kitagawa, *Cryst. Growth Des.*, 2013, **13**, 981; (b) M. G. Goesten, F. Kapteijn and J. Gascon, *CrystEngComm*, 2013, **15**, 9249; (c) M. Du, Z. Zhang, C. Li, J. Ribas-Ariño, N. R. Aliaga-Alcalde and J. Ribas, *Inorg. Chem.*, 2011, **50**, 8451; (d) B. Li, R. Wei, J. Tao, R. Huang, L. Zheng and Z. Zheng, *J. Am. Chem. Soc.*, 2010, **132**, 1558; (e) S. Y. Lee, J. H. Jung, J. J. Vittal and S. S. Lee, *Cryst. Growth Des.*, 2010, **10**, 1033; (f) Q. Chu, G. Liu, T. Okamura, Y-Q. Huang, W. Sun and N. Ueyama, *Polyhedron*, 2008, **27**, 812; (g)

Y. Zheng, M. Tong and X.-M. Chen, *New J. Chem.*, 2004, **28**, 1412; (h) M. Tong, X. Chen and S. R. Batten, *J. Am. Chem. Soc.*, 2003, **125**, 16170.

7. (a) Z. Zhang, J. Ma, Y. Liu, W. Kan and J. Yang, *Cryst. Growth Des.*, 2013, **13**, 4338; (b) X. Zhang, L. Fan, Z. Sun, W. Zhang, D. Li, J. Dou and L. Han, *Cryst. Growth Des.*, 2013, **13**, 792; (c) D. Sun, L. Han, S. Yuan, Y. Deng, M. Xu and D. Sun, *Cryst. Growth Des.*, 2013, **13**, 377; (d) L. Fan, X. Zhang, Z. Sun, W. Zhang, Y. Ding, W. Fan, L. Sun, X. Zhao and H. Lei, *Cryst. Growth Des.*, 2013, **13**, 2462; (e) M. Du, C. Li, C. Liu and S. Fang, *Coord. Chem. Rev.*, 2013, **257**, 1282; (f) F. Guo, F. Wang, H. Yang, X. Zhang and J. Zhang, *Inorg. Chem.*, 2012, **51**, 9677; (g) X. Shi, X. Wang, L. Li, H. Hou and Y. Fan, *Cryst. Growth Des.*, 2010, **10**, 2490. (h) J.-S. Hu, Y. Shang, X. Yao, L. Qin, Y. Li, Z. Guo, H. Zheng and Z. Xue, *Cryst. Growth Des.*, 2010, **10**, 4135; (i) He, D. Collins, F. Dai, X. Zhao, G. Zhang, H. Ma and D. Sun, *Cryst. Growth Des.*, 2010, **10**, 895; (j) Z. Li, J. Zhao, E. C. Sañudo, H. Ma, Z.-D. Pan, Y. Zeng and X. Bu, *Inorg. Chem.*, 2009, **48**, 11601. (k) Y. Qi, Y. Che and J.-M. Zheng, *Cryst. Growth Des.*, 2008, **8**, 3602; (l) P. Mahata,; G. Madras; S. Natarajan, *J. Phys. Chem. B*, 2007, **110**, 13759.

8. (a) H. Wu, J. Yang, Z. Su, S. R. Batten and J. Ma, *J. Am. Chem. Soc.*, 2011, **133**, 11406; (b) S.-S. Chen, M. Chen, S. Takamizawa, P. Wang, G. Lva and W. Sun, *Chem. Commun.*, 2011, **47**, 4902; (c) Z. Li, T. Hu, H. Ma, Y. Zeng, C. Li, M. Tong and X. Bu, *Cryst. Growth Des.*, 2010, **10**, 1138; (d) X. Wang, Y. Lv, T. Okamura, H. Kawaguchi, G. Wu, W. Sun and N. Ueyama, *Cryst. Growth Des.*, 2007, **7**, 1125; (e) J. Fan, G. T. Yee, G. Wang and B. E. Hanson, *Inorg. Chem.*, 2006, **45**, 599; (f) W. Zhao, J. Fan, T. Okamura, W. Sun and N. Ueyama, *Microporous And Mesoporous Materials*, 2005, **78**, 265; (g) G. Cui, J. Li, J. Tian, X. Bu and S. R. Batten, *Cryst. Growth Des.*, 2005, **5**, 1775; (h) S. Wan, Y. Huang, Y. Li and W. Sun, *Microporous and Mesoporous Materials*, 2004, 101; (i) S. Wan, Y. Li, T. Okamura, J. Fan, W. Sun and N.

Ueyama, *Eur. J. Inorg.*, 2003, 3783; (j) J. Fan, M. Shu, T. Okamura, Y. Li, W. Sun, W. Tang and N. Ueyama, *New J. Chem.*, 2003, **27**, 1307; (k) H. Liu, W. Sun, D. Ma, K. Yub and W. Tang, *Chem. Commun.*, 2000, 591.

9. (a) M. Lammert, S. Bernt, F. Vermoortele, D. E. De Vos and N. Stock, *Inorg. Chem.*, 2013, **52**, 8521; (b) L. Jia, L. Hou, L. Wei, X. Jing, B. Liu, Y. Wang and Q. Shi, *Cryst. Growth Des.*, 2013, **12**, 1570; (c) Y. Xue, F. Jin, L. Zhou, M. Liu, Y. Xu, H. Du, M. Fang and X. You, *Cryst. Growth Des.*, 2012, **12**, 6158; (d) X. Lin, I. Telepeni, A. J. Blake, A. Dailly, C. M. Brown, J. M. Simmons, M. Zoppi, G. S. Walker, K. M. Thomas, T. J. Mays, P. Hubberstey, N. R. Champness and M. Schröder, *J. Am. Chem. Soc.*, 2009, **131**, 2159; (e) H. Choi and M. P. Suh, *Angew. Chem. Int. Ed.*, 2009, **48**, 6865; (f) A. D. Burrows, C. G. Frost, M. F. Mahon and C. Richardson, *Chem. Commun.*, 2009, 4218; (g) P. D. C. Dietzel, R. E. Johnsen, R. Blom and H. Fjellvåg, *Chem. Eur. J.*, 2008, **14**, 2389. (h) D. Xiao, Y. Li, E. Wang, L. Fan, H. An, Z. Su and L. Xu, *Inorg. Chem.*, 2007, **46**, 4158.

10. (a) J. Zhou, L. Du, Y. Qiao, Y. Hu, B. Li, L. Li, X. Wang, J. Yang, M. Xie and Q. Zhao, *Cryst. Growth Des.*, 2014, **14**, 1175; (b) Y. Mu, X. Ma, B. Han, G. Qin, Y. Niu and H. Lü, *Polyhedron*, 2014, **67**, 44; (c) A. Li, Q. Guo, L. Li, H. Hou and Y. Fan, *Polyhedron*, 2014, **71**, 17; (d) S. Mukherjee, D. Samanta and P. S. Mukherjee, *Cryst. Growth Des.*, 2013, **13**, 5335; (e) M. Du, X. Jiang and X. Zhao, *Inorg. Chem.*, 2007, **46**, 3984.

11. (a) K. Binnemans, *Chem. Rev.*, 2009, **109**, 4283; (b) M. D. Allendorf, C. A. Bauer, R. K. Bhakta and R. J. T. Houk, *Chem. Soc. Rev.*, 2009, **38**, 1330.

12. (a) L. S. D. Carlos, R. A. S. Ferreira, V. D. Z. Bermudez, B. Julian-Lopezc and P. Escribano, *Chem. Soc. Rev.*, 2011, **40**, 536; (b) S. V. Eliseevaa and J. G. Bunzli, *Chem. Soc. Rev.*, 2010, **39**, 189; (c) S. Hwang, C. N. Moorefield and G. R. Newkome, *Chem. Soc. Rev.*,

2008, **37**, 2543; (d) J. E. McGarrah, Y. Kim, M. Hissler and R. Eisenberg, *Inorg. Chem.*, 2001, **40**, 4510; (e) Q. Wu, M. Esteghamatian, N.-. Hu, Z. Popovic, G. Enright, Y. Tao, M. D'Iorio and S. Wang, *Chem. Mater.*, 2000, **21**, 79.

13. (a) S. V. Rocha and N. S. Finney, *J.Org. Chem.*, 2013, **18**, 11255; (b) S. V. Rocha and N. S. Finney, *Org. Lett.*, 2010, **12**, 2598.

14. N. Singh and G. Anantharaman, *CrystEngComm*, 2014, DOI: 10.1039/C1034CE00691G

15. B. S. Furniss, A. J. Hannaford, P. W. G. Smith and A. R. Tatchell, *VOGEL's Textbook of Practical Organic Chemistry*, 5th edn., *Pearson Education*, Longman Group UK, 2005.

16. W. Madison, *Saint software refrence manual*, 1998.

17. G. M. Sheldrick, SHELXL-97, *Program for Crystal Structure Solution and Refinement*, University of Göttingen, Göttingen, Germany, 1997.

18. A. L. Spek, *Acta Cryst.* 2009, **D65**, 148-155

19. (a) K. Nakamoto, *Infrared and Raman Spectra of Inorganic and Coordination Compounds Part B*, 6th edn., *Wiley, New York*, 1986; (b) G. B. Deacon and R. J. Phillips, *Coord.Chem.Rev*, 1980, **33**, 227.

20. (a) S. Li, Y. Lan, J. Ma, J. Yang, G. Wei, L. Zhang and Z. Su, *Cryst. Growth Des*, 2008, **8**, 675; (b) S. G. Baca, I. G. Filippova, N. V. Gerbeleu, Y. A. Simonov, M. Gdaniec, G. A. Timco, O. A. Gherco and Y. L. Malaestean, *Inorg. Chim. Acta*, 2003, **344**, 109.

21. J. Song, Y. Chen, Z. Li, R. Zhou, X. Xu and J. Xu, *J. Mol. Struct.*, 2007, **842**, 125.

22. (a) Y. Qi, F. Luo, Y. Che and J. Zheng, *Cryst. Growth Des.*, 2008, **8**, 606; (b) Y.-Y. Liu, J.-F. Ma, J. Yang and Z. Su, *Inorg. Chem.*, 2007, **46**, 3027.

23. (a) X. Zhang, W. Song, Q. Yang and X. Bu, *Dalton Trans.*, 2012, **41**, 4217; (b) C. Qin, X. Wang, E. Wang, Y. Qi, H. Jin, S. Chang and L. Xu, *J. Mol. Struct.*, 2005, **749**, 138.

24. (a) W. Zhao, Y. Song, T. Okamura, J. Fan, W. Sun and N. Ueyama, *Inorg. Chem.*, 2005, **44**, 3330; (b) L. Zhang, M. Zeng, X. Sun, Z. Shi, S. Feng and X. Chen, *J. Mol. Struct.*, 2004, **697**, 181.

25. (a) H. Jiang, B. Liu and Q. Xu, *Cryst. Growth Des.*, 2010, **10**, 806; (b) X. Li, X. Wang and Y. Zhang, *Inorg. Chem. Commun*, 2008, **11**, 832.

26. (a) H. A. Habib, A. Hoffmann, H. A. Hoppea and C. Janiak, *Dalton Trans.*, 2009, 1742; (b) P. Ren, M. Liu, J. Zhang, W. Shi, P. Cheng, D. Liao and S.-P. Yan, *Dalton Trans.*, 2008, 4711.

27. (a) Y. Yang, P. Du, Y. Liu and J. Ma, *Cryst. Growth Des.*, 2013, **13**, 4781; (b) Z. Shi, Y. Li, Z. Guo and H. Zheng, *Cryst. Growth Des.*, 2013, **13**, 3078.

28. S. Zheng, J. Yang, X. Yu, X. Chen and W. Wong, *Inorg. Chem.*, 2004, **43**, 830.

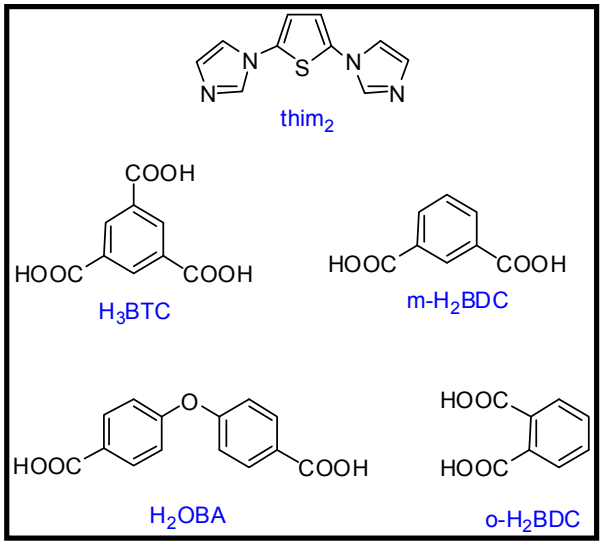

Scheme 1 N-donor $thim_2$ ligand and O-donor carboxylate based coligands

Table 1. Crystal data and structure refinement parameters for **1-7**

Compound	**1**	**2**	**3**	**4**	**5**	**6**	**7**
Formula	$C_{18}H_{16}N_4O_6SZn$	$C_{18}H_{12}N_4O_4SCo$	$C_{19}H_{14}N_4O_7SCo$	$C_{19}H_{14}N_4O_7SZn$	$C_{24}H_{20}N_4O_7SCo$	$C_{24}H_{20}N_4O_7SZn$	$C_{36}H_{26}N_8O_9S_2Mn_2$
Formula wt.	481.80	439.31	501.33	507.79	567.43	573.87	888.65
Space group	*P*2(1)/*n*	*P*2(1)2(1)2(1)	*P*2(1)/*n*	*P*2(1)/*n*	*C*2/*c*	*C*2/*c*	*P*-1
a (Å)	9.961(5)	10.1448(12)	7.2476(6)	7.2709(15)	28.205(6)	28.266(6)	9.611(4)
b (Å)	17.323(4)	11.9933(14)	17.4087(15)	17.234(3)	12.181(2)	12.094(2)	10.082(5)
c (Å)	10.814(5)	13.9849(16)	15.9969(14)	16.173(3)	15.442(3)	15.364(3)	18.355(5)
α, deg	90.000	90.000	90.000	90.000	90.000	90.000	80.514(5)
β, deg	94.871(5)	90.000	90.364(2)	90.215(4)	108.09(3)	107.51(3)	85.412(3)
γ, deg	90.000	90.000	90.000	90.000	90.000	90.000	82.853(5)
V/Å^3	1859.3(13)	1701.5(3)	2018.3(3)	2026.6(7)	5043.1(17)	5009.0(17)	1737.4(12)
Z	4	4	4	4	8	8	2
D_{calcd} g/cm^3	1.707	1.715	1.643	1.658	1.495	1.522	1.699
μ, mm^{-1}	1.480	1.167	1.006	1.367	0.815	1.116	0.919
F(000)	968	892	1012	1024	2328	2352	904
Reflns collected	10388	9196	14035	11308	12911	17616	9614
Indep. Reflns	3647	3161	3959	3958	4442	4911	6643
GOF	1.118	1.097	1.032	1.084	1.091	0.980	1.072
R_1/ wR_2 [I >2σ(I)]	0.0527, 0.1315	0.0372, 0.0841	0.0680, 0.1669	0.0738, 0.1935	0.0431, 0.1155	0.0529, 0.1108	0.0529, 0.1219
R_1/ wR_2 (all data)	0.0740, 0.1822	0.0439, 0.0908	0.1036, 0.1904	0.1077, 0.2412	0.0549, 0.1334	0.0874, 0.1207	0.0751, 0.1419
Flack Value		0.456(18)					

Table 2. M-M distances and dihedral angle table for **1-6**

CP	Distance between M-M connected by thim$_2$ (Å)	Dihedral angle between two imidazole units (^{o})	Distance between M-M connected by Carboxylate co-ligand (Å)	Dihedral angle between two coordinated carboxylates units (^{o})
2	12.19	87.01 (9)	10.14	12.77 (1)
4	12.40	60.32 (2)	9.18	17.31 (6)
3	12.40	66.31 (8)	9.07	20.76 (2)
1	12.55	48.48 (9)	7.28	58.72 (1)
5	13.81	72.25 (3)	12.18	59.99 (2)
6	13.09	74.29 (4)	12.09	67.56 (3)

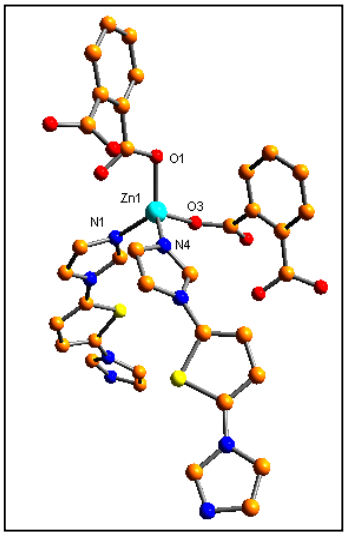

(a)

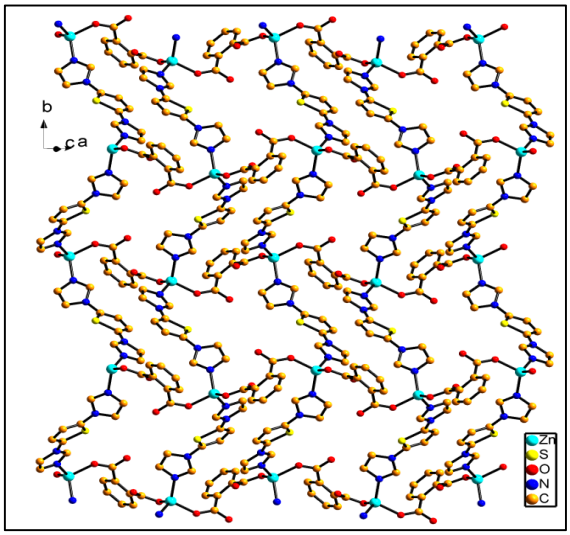

(b)

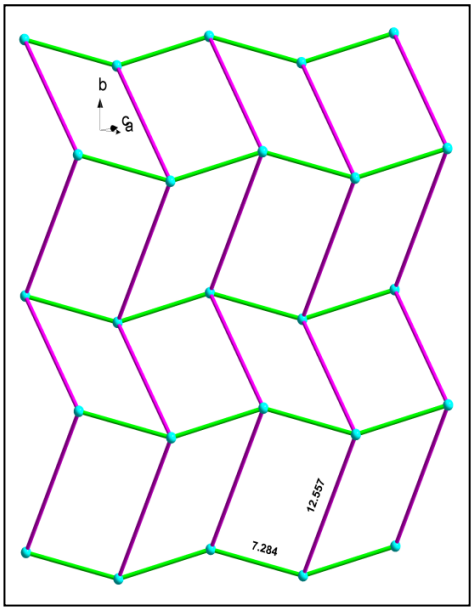

(c)

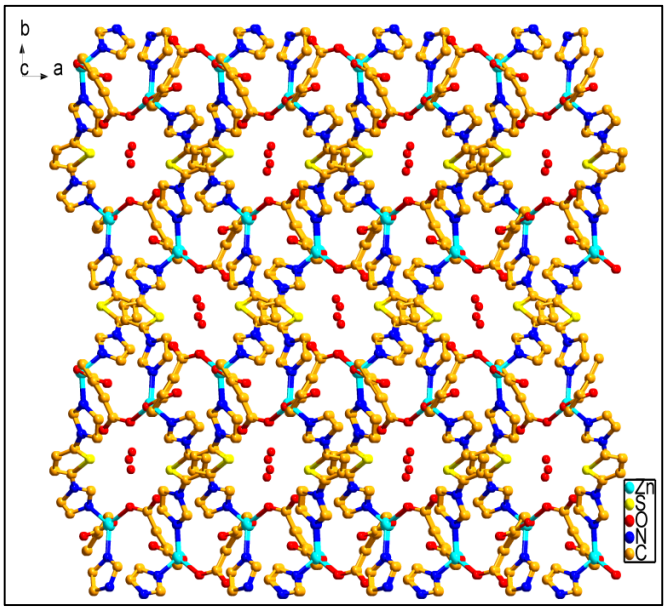

(d)

Figure 1.

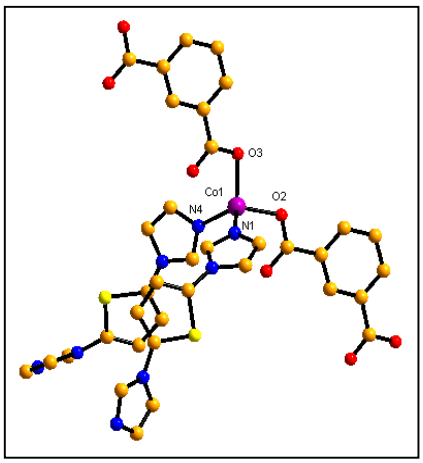

(a)

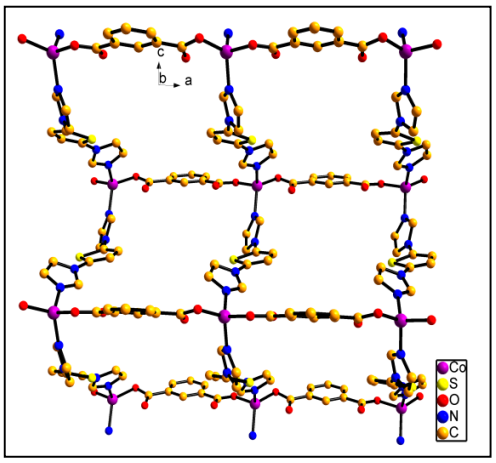

(b)

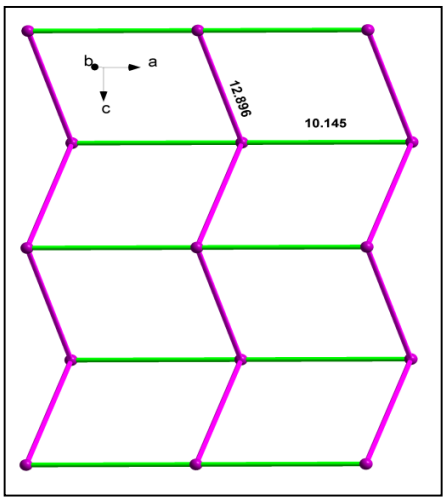

(c)

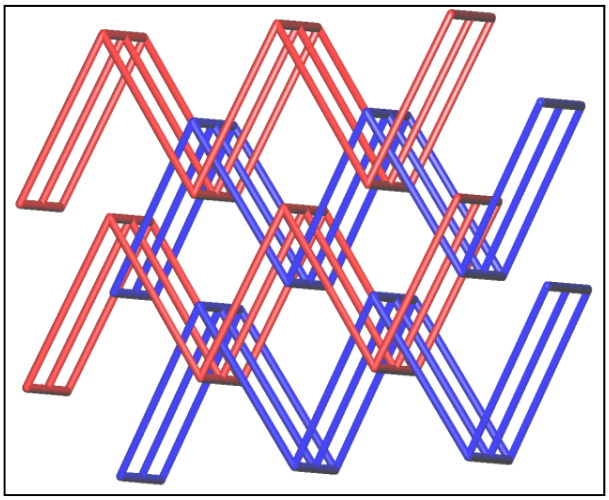

(d)

Figure 2

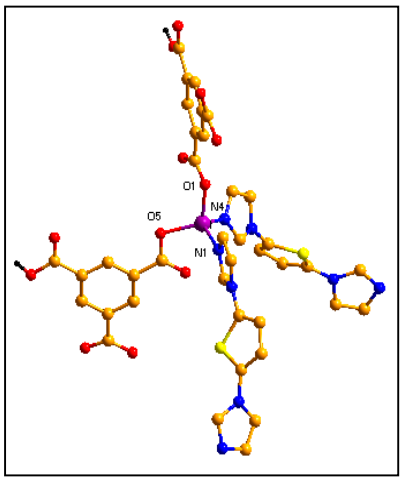

(a)

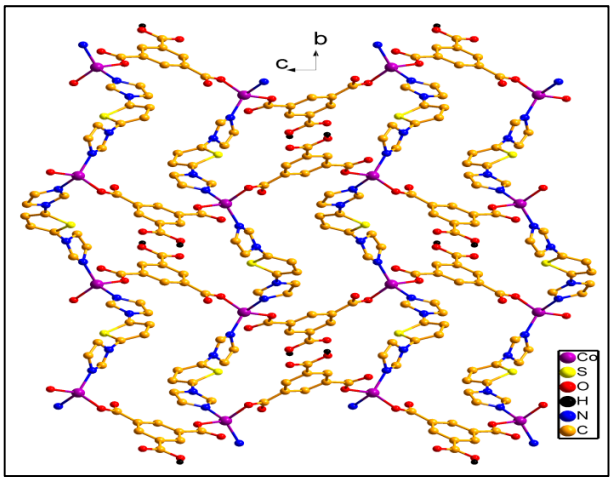

(b)

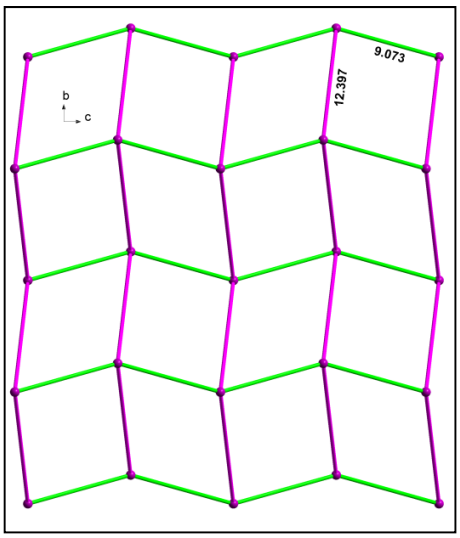

(c)

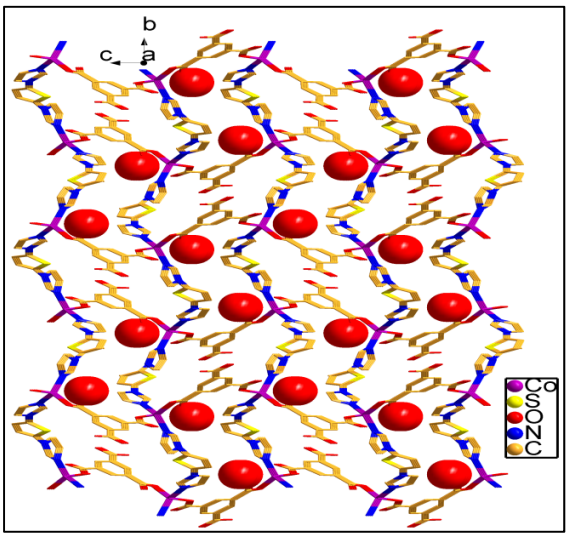

(d)

Figure 3.

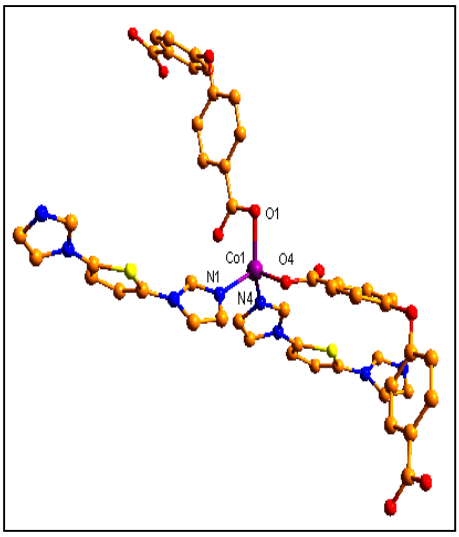

(a)

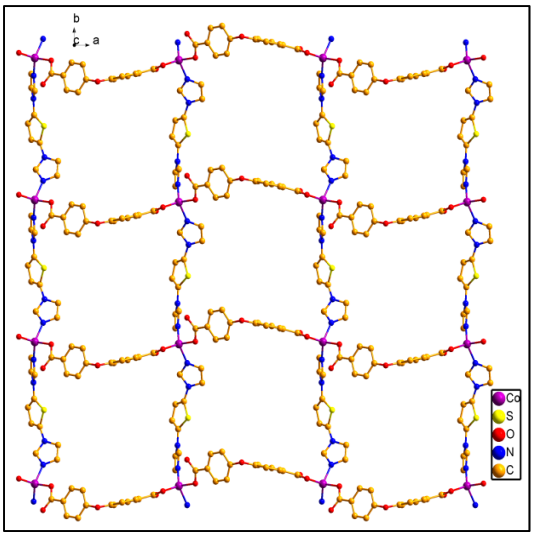

(b)

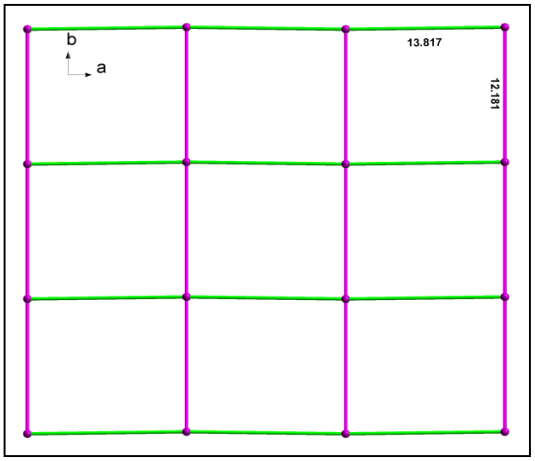

(c)

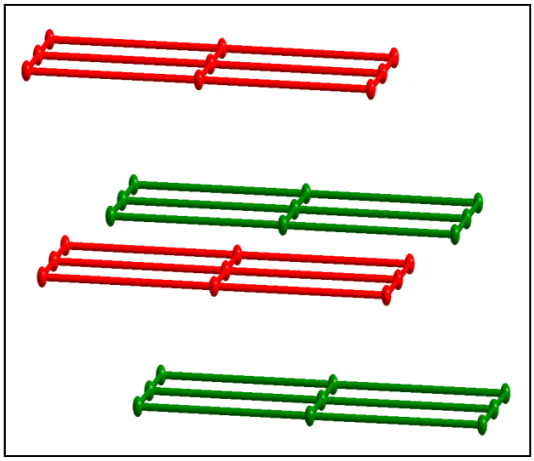

(d)

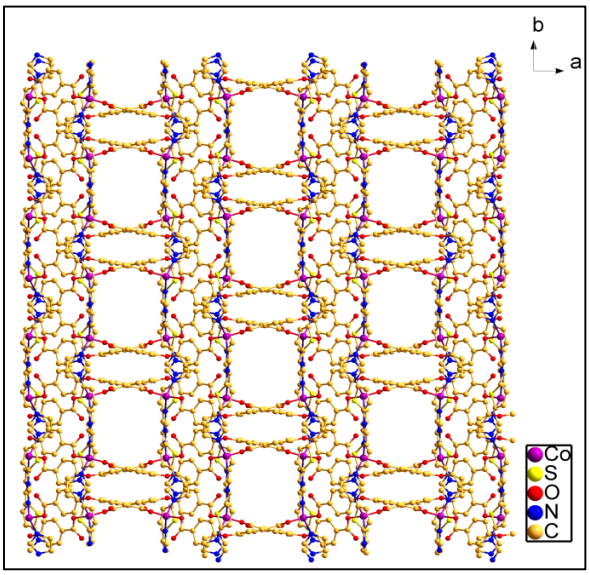

(e)

Figure 4

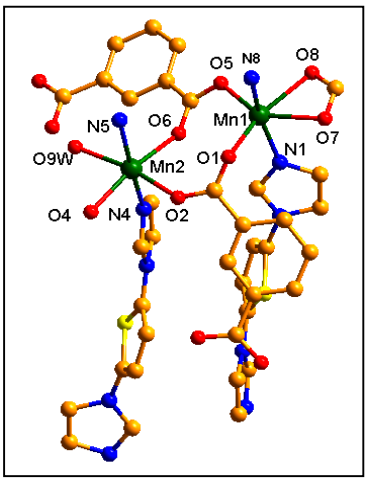

(a)

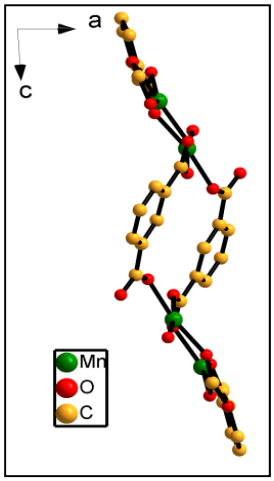

(c)

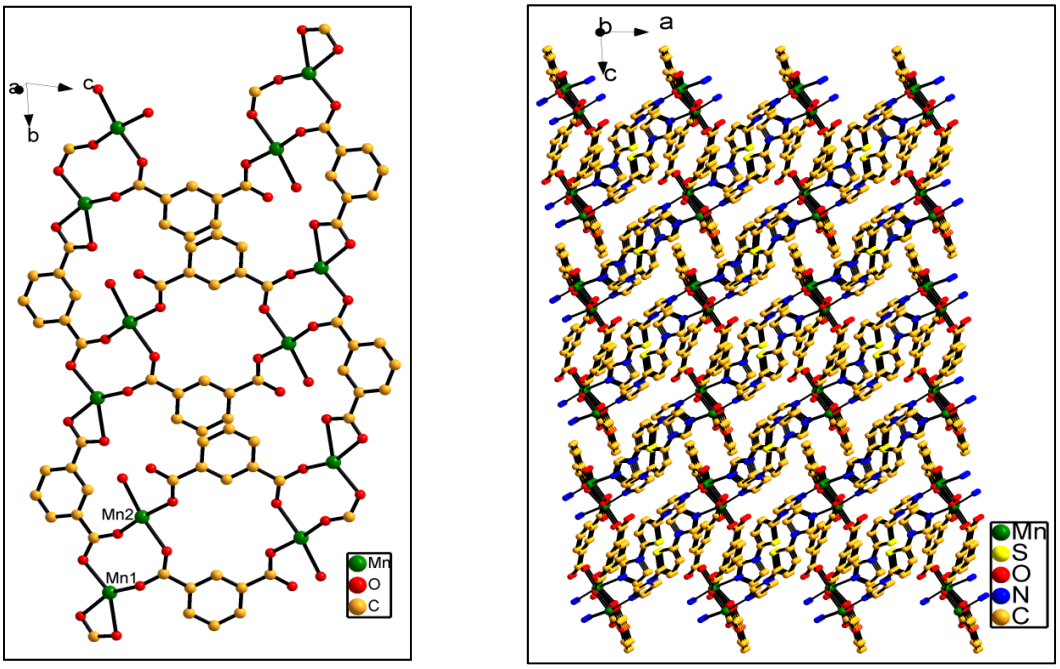

(b) (d)

Figure 5.

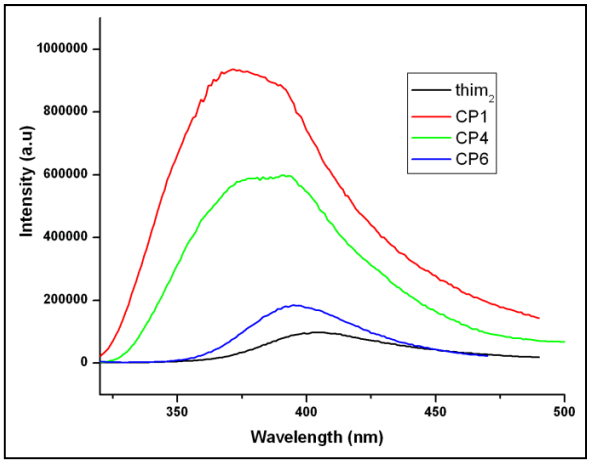

Figure 6

Captions for the Figures

Figure 1	(a) Coordination environment surrounding Zn(II) in **1** (b)View of the 2D herringbone pleated network along the *c* axis (c) Topological representation of the 2D herringbone pleated network (d) 3D view of **1** with solvent molecules.
Figure 2	(a) Coordination environment surrounding Co(II) in **2** (b) View of the 2D parallel pleated network (c) Topological representation of the 2D parallel pleated network (d) Topological representation of the 2D+2D= 3D polycatenated network
Figure 3	(a) Coordination environment surrounding Co(II) in **3** (b)View of the 2D herringbone pleated network along the *a* axis (c) Topological representation of the 2D herringbone pleated network (d) 3D view of **3** with solvent molecules.
Figure 4	(a) Coordination environment surrounding Co(II) in **5** (b) View of the 2D grid along the *c* axis (c) Topological representation of the 2D layer (d) Topological representation of the *ABAB* pattern (e) Packed 3D supramolecular architecture of **5**
Figure 5	(a) Coordination environment surrounding Mn(II) in **7** (b) View of the 1D double chain along the *a* axis. (c) View of the 1D double chain along the *b* axis (d)3D network of **7**
Figure 6	Solid state emission spectra at room temperature

For the Table of Contents only

Structural Diversity and Luminescent Properties of Coordination Polymers Based on 2,5-Bis(Imidazol-1-yl)Thiophene ($Thim_2$) and Aromatic Multicarboxylates

Namita Singh and Ganapathi Anantharaman*

Department of Chemistry, Indian Institute of Technology (IIT), Kanpur – 208016, INDIA.

Email: garaman@iitk.ac.in.

Seven new CPs, exhibiting 2D harringbone pleated (**1**, **3**-**4**), parallel pleated (**2**), layer (**5**-**6**) structure and 3D nework (**7**) have been synthesized. Solid-state photoluminescence property for CP **1, 4** and **6** has been investigated.